DALTON

Electrochemistry of molybdenum imides: cleavage of molybdenum–nitrogen triple bonds to release ammonia or amines †

Yatimah Alias,[a] Saad K. Ibrahim,[a] M. Arlete Queiros,[b] Antonio Fonseca,[b] Jean Talarmin,[c] Florence Volant[a,c] and Christopher J. Pickett*[,a]

[a] *The Nitrogen Fixation Laboratory, John Innes Centre, Norwich Research Park, Colney, Norwich, UK NR4 7UH*
[b] *Departamento de Química, Escola de Ciências, Universidade do Minho, Campus de Gualtar, 4700 Braga, Portugal*
[c] *UMR CNRS 6521, Faculté des Sciences, Université de Bretagne Occidentale, BP 809, 29285 Brest, France*

The electrochemical reduction of molybdenum(IV) alkylimides *trans*-$[MoX(NR)(dppe)_2]^+$ (X = halide, R = alkyl, dppe = $Ph_2PCH_2CH_2PPh_2$) proceeded by two pathways. In the *absence* of a source of protons, moderately stable five-co-ordinate molybdenum(II) imides are formed *via* an initial single-electron transfer followed by rate-determining loss of the *trans*-halide ligand and an additional electron transfer. In the *presence* of a source of protons, molybdenum–halide bond cleavage is intercepted by protonation at N which gives an amide intermediate. Further electron-transfer chemistry liberates amines and yields a dinitrogen complex in an overall four-electron process. Molybdenum(IV) imides *trans*-$[MoX(NH)(dppe)_2]^+$ were reduced to amide intermediates with the parent imide cation providing the source of protons and water probably acts as a proton-transfer relay. The amide has two fates; it is either converted into a nitride by hydrogen loss or, at a potential which encompasses its further reduction, yields ammonia and a dinitrogen complex.

Methods for making organonitrogen compounds from molecular nitrogen *via* reactions at transition-metal centres are being actively explored in several laboratories and novel synthetic routes have been developed for functionalising dinitrogen ligands,[1–3] some of which exploit steric and/or electronic control of reactivity by the metal site.[4–6] A key element in much of this chemistry is the cleavage of a metal–nitrogen multiple bond to release the 'free' organonitrogen product. There are clear advantages if such cleavage reactions proceed under mild conditions without degradation of the metal site and this is likely to become especially important in the context of recycling metal/chiral auxillary ligand assemblies in asymmetric syntheses.[7]

There are principally two types of conserved metal–ligand 'platform' at which dinitrogen binds and also shows a wide and diverse N–C bond-forming chemistry. These are the tetrasulfur macrocycle[2,8] and bis(diphosphine) assemblies of molybdenum or tungsten.[1,3] At sites such as *trans*-$\{M(dppe)_2\}$ (M = Mo or W; dppe = $Ph_2PCH_2CH_2PPh_2$) molecular nitrogen can be converted into organohydrazines, amines, amino acids, N-heterocycles or nitriles by stepwise reactions involving the synthesis of stable diazenide, hydrazide, nitride or imide intermediates.[1,3,9] For example cleavage of the N–N bond in a molybdenum organohydrazide can be accomplished by successive electron- and proton-transfer steps to give an amine and a nitride, *trans*-$[MoX(N)(dppe)_2]$ (X = halide);[9] in turn, this type of nitride can be converted into organoimide cations such as *trans*-$[MoCl(NCHMeCO_2Me)(dppe)_2]^+$ by stepwise N–C and C–C bond-forming reactions;[10,11] from the organoimide, the nitrogen ligand can be electrochemically released as alanine methyl ester by reductive cleavage of the $\{Mo{\equiv}N^+\}$ triple bond.[10,11] Such Mo–N bond-cleavage reactions occur with conservation of the bis(diphosphine)molybdenum assembly and, under molecular nitrogen at 1 atm (*ca.* 101 325 Pa), *trans*-$[Mo(N_2)_2(dppe)_2]$ is generated in reasonable yields.[9]

† *Supplementary data available* (No. SUP 57309, 4 pp.): simulation parameters. See Instructions for Authors, *J. Chem. Soc.*, *Dalton Trans.*, 1997, Issue 1.

Multielectron reduction of organoimide cations *trans*-$[MoX(NR)(dppe)_2]^+$ (R = organic group) to give amines has a parallel in the reduction chemistry of related imide cations, *trans*-$[MoX(NH)(dppe)_2]^+$ because these can yield ammonia,[12] a reaction pathway of some interest in the context of nitrogen fixation by molybdenum nitrogenase.[13]

This paper describes the reductive electrochemistry of compounds of the type *trans*-$[MoX(NR)(dppe)_2]^+$ and *trans*-$[MoX(NH)(dppe)_2]^+$ and discusses mechanistic aspects of the multielectron transfer processes involved in the electrolytic cleavage of molybdenum–nitrogen triple bonds.

Results and Discussion

Organoimides

Cyclic voltammetry shows that the reduction of the organoimide cations *trans*-$[MoX(NR)(dppe)_2]^+$ is essentially an irreversible process at room temperature at vitreous carbon or platinum electrodes in dimethylformamide (dmf)–0.1 M $[NBu_4][BF_4]$ or other non-aqueous electrolytes at modest scan rates (< 100 mV s^{-1}). However, at low temperatures reversibility becomes evident. For example, at −36 °C in dmf–0.1 M $[NBu_4][BF_4]$, *trans*-$[MoCl(NEt)(dppe)_2]^+$ displays a partially reversible process with the magnitude of the peak current (i_p^{red}) and the separation of the peak potentials (ΔE) close to those observed for the (known) reversible one-electron oxidation of an equimolar solution of *trans*-$[Mo(N_2)_2(dppe)_2]$ recorded under identical conditions, Fig. 1. This is consistent with the primary reduction of *trans*-$[MoCl(NEt)(dppe)_2]^+$ involving a single-electron transfer step, equation (1), in agreement with

$$trans\text{-}[MoX(NR)(dppe)_2]^+ \underset{-e}{\overset{+e}{\rightleftharpoons}} trans\text{-}[MoX(NR)(dppe)_2] \quad \text{(unstable)} \qquad (1)$$

earlier ultramicroelectrode studies of *trans*-$[MoCl(NMe)(dppe)_2]^+$ on mercury at low temperature.[14] Partially reversible

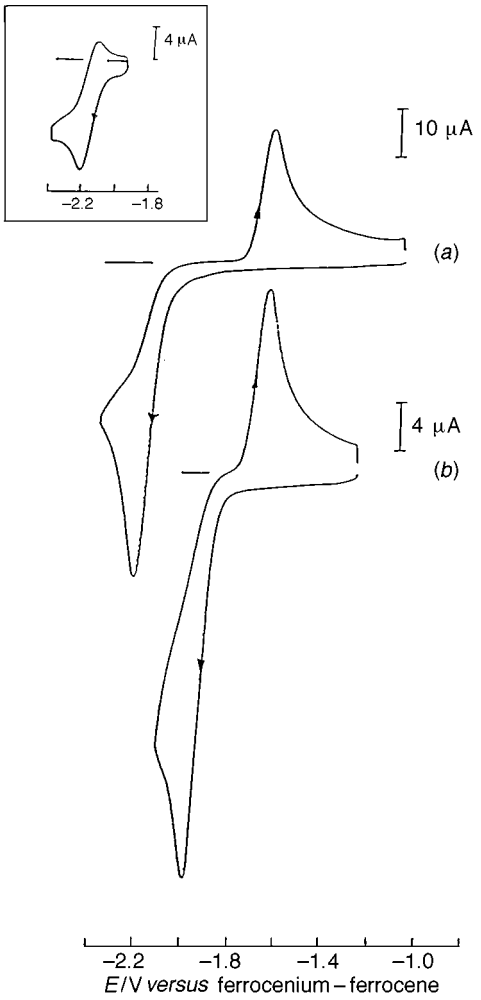

Fig. 1 Cyclic voltammograms: (*a*) *trans*-$[MoCl(NEt)(dppe)_2]^+$ (3.3 mM) in dmf–0.1 M $[NBu_4][BF_4]$ at 25 °C, scan rate 100 mV s^{-1}, the inset shows the reversible behaviour of the system at −36 °C; (*b*) *trans*-$[MoI(NEt)(dppe)_2]^+$ (1.7 mM) under same conditions as for (*a*)

single-electron transfer is observed for other organoimide complexes *trans*-$[MoX(NR)(dppe)_2]^+$ [X = Cl or Br; R = CH_2CO_2Me, $CH(Me)CO_2Me$, CH_2Ph, CH(Me)Ph, CH=CHMe or $CH_2CH{=}CH_2$] at low temperature.

The single-electron reduction of the molybdenum(IV) alkylimide cations give neutral intermediates which are formally in oxidation state III. If the Mo–N–C framework remains linear with sp-hybridised N, then the intermediate has a 19-electron configuration. Conversely, if a *bent* geometry with sp^2 hybridisation at N is adopted then a 17-electron configuration is achieved, Scheme 1 (see below). There is considerable precedence for ligand rearrangement when this is necessary to accommodate electron addition to a closed-shell complex. Perhaps the best analogy is the change from a linear MoNO bonding mode to the bent conformation upon one-electron reduction of 18-electron molybdenum cyclopentadienyl nitrosyl compounds as reported by Geiger *et al.*[14] The lowest unoccupied molecular orbital (LUMO) in the nitrosyl system is believed to have predominately Mo–NO σ* antibonding character.[15] The LUMO of the Mo–NR complexes may similarly possess Mo–NR σ* character, however the dependence of the reduction potential on the nature of the *trans*-halide ligand in the alkylimide complexes suggests that Mo–X interactions may also contribute to the LUMO.

The chemistry following the primary electron-transfer reaction of *trans*-$[MoX(NR)(dppe)_2]^+$ leads to further electron transfer and the formation of a moderately stable five-coordinate, closed-shell molybdenum(II) product, *trans*-$[Mo(NR)(dppe)_2]$, equation (2). The evidence for the formation of the

Table 1 Peak potentials for irreversible oxidation of *trans*-$[Mo(NR)(dppe)_2]$ recorded in thf–0.2 M $[NBu_4][BF_4]$ at a vitreous carbon electrode, at 100 mV s^{-1} and 0 °C. Potentials are relative to ferrocenium–ferrocene

R	E_p^{ox}/V
Me	−1.50
Et	−1.51
Pr^i	−1.61
$CH_2CH{=}CH_2$	−1.43
CH_2Ph	−1.52
$CH_2C_{10}H_7$	−1.48
CH(Me)Ph	−1.58

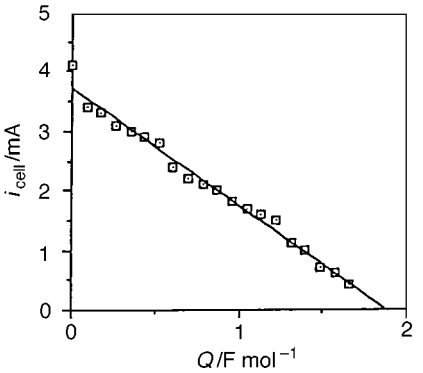

Fig. 2 Current *versus* charge passed for reduction of *trans*-$[MoCl(NEt)(dppe)_2]^+$ at mercury-pool cathode at 0 °C in dmf–0.1 M $[NBu_4][BF_4]$ at $E_{applied}$ = −2.3 V

$$trans\text{-}[MoX(NEt)(dppe)_2]^+ \xrightarrow{+2e} trans\text{-}[Mo(NEt)(dppe)_2] + X^- \quad (2)$$

five-co-ordinate species is as follows. Fig. 1(*a*) shows a typical cyclic voltammogram of *trans*-$[MoCl(NEt)(dppe)_2]^+$ recorded at 25 °C in dimethylformamide (dmf)–0.1 M $[NBu_4][BF_4]$ at a vitreous carbon electrode. The reduction process at E_p^{red} = −2.21 V *versus* ferrocenium–ferrocene leads to the generation of a product which is detected on the reverse scan by its oxidation near −1.6 V. The peak-current function is independent of potential scan rate (ν) in the range 10 to 100 mV s^{-1} and corresponds to a diffusion-controlled two-electron reduction. The peak potential for the reduction of the iodo-complex, *trans*-$[MoI(NEt)(dppe)_2]^+$, occurs at a potential some 200 mV *positive* of E_p^{red} for the chloro-species; however, the oxidation potential of the product is *the same as that for the species generated from the chloro-analogue*, Fig. 1(*b*). This is consistent with cleavage of the metal–halide bond giving rise to the same product, *trans*-$[Mo(NEt)(dppe)_2]$, equation (2). The release of halide following reduction of *trans*-$[MoI(NEt)(dppe)_2]^+$ was confirmed by observation of the characteristic oxidative response of free iodide upon scan reversal.

The peak potential for the oxidation of the two-electron product is essentially insensitive to the nature of the solvent, dmf, methyl cyanide or tetrahydrofuran (thf) as is consistent with the absence of solvent co-ordination at the vacated halide site. Conservation of the nitrogen ligand upon reduction is evident from the dependence of E_p^{ox} of the product on R when generated from other *trans*-$[MoCl(NR)(dppe)_2]^+$, Table 1.

Controlled-potential reduction of *trans*-$[MoCl(NEt)(dppe)_2]^+$ at or below 0 °C in the dmf electrolyte affords a moderately stable solution of *trans*-$[Mo(NEt)(dppe)_2]$. Thus exhaustive electrolysis at −2.3 V *versus* ferrocenium–ferrocene on a mercury-pool cathode in the dmf electrolyte at 0 °C is an overall two-electron process, as shown by the cell current *versus*

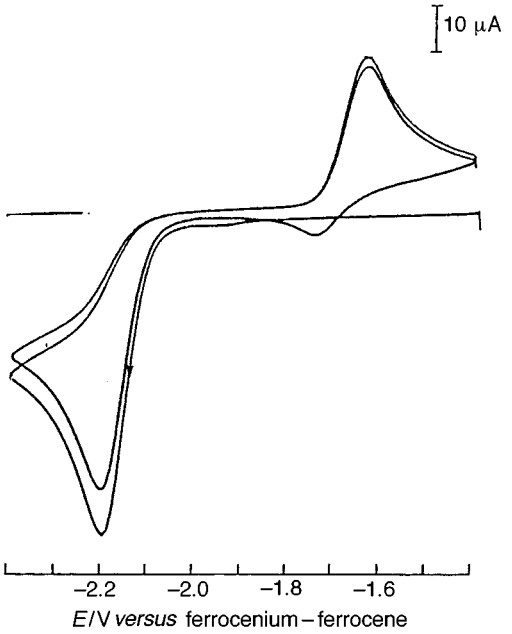

Fig. 3 Cyclic voltammogram of *trans*-$[MoCl(NEt)(dppe)_2]^+$ in dmf–0.1 M $[NBu_4][BF_4]$ at a vitreous carbon electrode. Scan rate 50 mV s^{-1}; 0 °C. The first and second scans are shown

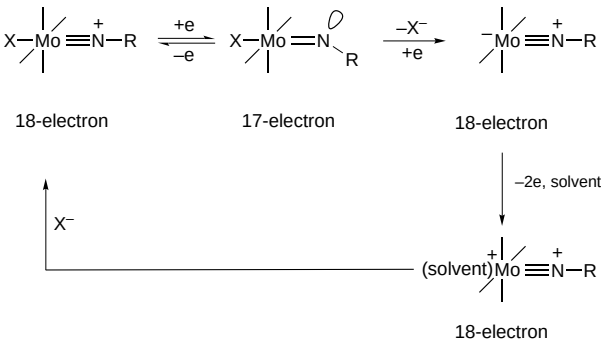

Scheme 1

charge passed plot of Fig. 2. Cyclic voltammetry after electrolysis shows that the five-co-ordinate product is formed as the major electroactive species. A small amount (≈10%) of the ylide *trans*-$[MoCl(NCHMe)(dppe)_2]$ is also produced by deprotonation of the parent complex at the α-carbon (see below). The ^{31}P-$\{^1H\}$ NMR spectrum of the catholyte solution after exhaustive electrolysis at or below 0 °C shows a major singlet at δ −53.8 relative to trimethyl phosphite (tmp). This is in accord with a square-planar arrangement of the phosphine ligands with the imide group occupying the apical position of a square pyramid. That the resonance is a singlet also implies that the imide group is linear, with sp-hybridised N providing a stable eighteen-electron configuration.

Consistent with the five-co-ordinate geometry, two-electron irreversible *oxidation* of *trans*-$[Mo(NEt)(dppe)_2]$ and concomitant ligation by a solvent molecule or an anion gives six-co-ordinate closed-shell cations. Fig. 3 shows a cyclic voltammogram of *trans*-$[MoCl(NEt)(dppe)_2]^+$ recorded in dmf–0.1 M $[NBu_4][BF_4]$ which encompasses a second cycle. The irreversible oxidation of *trans*-$[Mo(NEt)(dppe)_2]$ generates a new species *trans*-$[Mo(NEt)(solvent)(dppe)_2]^{2+}$ which reduces irreversibly with $E_p = -1.75$ V. In an MeCN electrolyte, the reduction peak of the product is shifted to $E_p = -1.67$ V. Examination of the cyclic voltammetry of an electrogenerated solution of *trans*-$[Mo(NEt)(dppe)_2]$ in dmf–0.1 M $[NBu_4][BF_4]$ shows that the irreversible two-electron oxidation leads to both the formation of *trans*-$[Mo(NEt)(solvent)(dppe)_2]^{2+}$ *and* to the regeneration of the starting material, *trans*-$[MoCl(NEt)(dppe)_2]^+$. Moreover, addition of free chloride ion to the electrolyte suppresses the peak arising from the reduction of *trans*-$[Mo(NEt)(solvent)(dppe)_2]^{2+}$ and enhances that due to *trans*-$[MoCl(NEt)(dppe)_2]^+$. The overall electrochemistry of *trans*-$[MoX(NEt)(dppe)_2]^+$ (X = Cl or I) and by analogy that of other alkylimide derivatives is thus far summarised by Scheme 1.

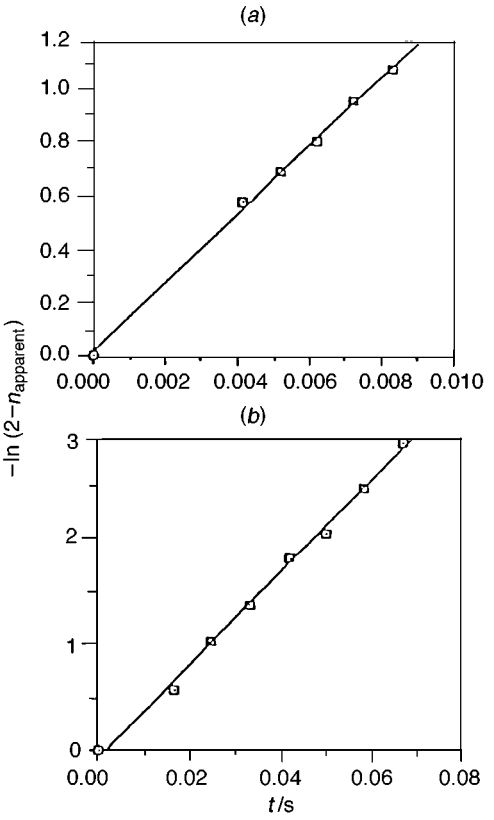

Fig. 4 Determination of the rate constant for halide loss from *trans*-$[MoCl(NEt)(dppe)_2]$: (*a*) $-\ln(2 - n_{apparent})$ *versus* time (*t*) plot for X = Cl; (*b*) as above for X = I. Data obtained by chronoamperometry in dmf–0.1 M $[NBu_4][BF_4]$ at 0 °C

The observation of partial reversibility of the organoimide systems at low temperature and their two-electron reduction at ambient temperature, equations (1) and (2), is in accord with halide loss constituting the intervening chemical step in an overall electrochemical step–chemical step–electrochemical step (e.c.e.) mechanism, equations (3) and (4). The magnitude of k_f,

$$trans\text{-}[MoX(NEt)(dppe)_2] \xrightarrow{k_f} trans\text{-}[Mo(NEt)(dppe)_2]^+ + X^- \quad (3)$$

$$trans\text{-}[Mo(NEt)(dppe)_2]^+ \underset{-e}{\overset{+e}{\rightleftharpoons}} trans\text{-}[Mo(NEt)(dppe)_2] \quad (4)$$

equation (3), was determined by chronoamperometry and by cyclic voltammetry. Data from chronoamperometric experiments were analysed using the relationship[15] (5) which for

$$(it^{\frac{1}{2}})_{obs}/2(it^{\frac{1}{2}})_{k=0} = 1 - [n_2/(n_1 + n_2)] \exp -k_f t \quad (5)$$

$n_1 = n_2 = 1$ reduces to that equation (6). Fig. 4 shows a plot of

$$n_{apparent} = 2 - \exp -k_f t \quad (6)$$

data obtained at 0 °C for *trans*-$[MoCl(NEt)(dppe)_2]^+$ in dmf–0.1 M $[NBu_4][BF_4]$ at a vitreous carbon electrode: the correlation coefficient for the $-\ln(2 - n_{apparent})$ *vs.* *t* plot is 0.999. The rate

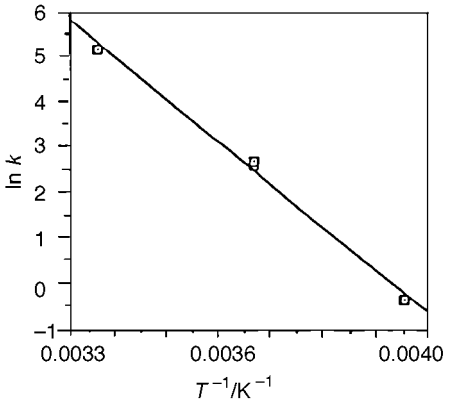

Fig. 5 Arrhenius plot for reaction of *trans*-[MoCl(NEt)(dppe)$_2$] to *trans*-[Mo(NEt)(dppe)$_2$]$^+$. Data obtained in dmf–0.1 M [NBu$_4$][BF$_4$] at 0 °C. $E_a = 76 \pm 5$ kJ mol^{-1}

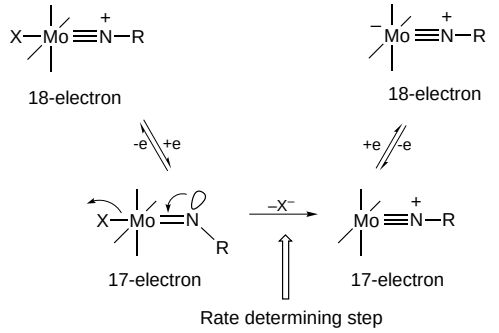

Scheme 2

constant, k_f^{Cl}, was calculated from the slope to be 14 ± 0.5 s^{-1} which is in good agreement with 15 ± 2 s^{-1} estimated independently from cyclic voltammetric data, Fig. 4.‡ A corresponding chronoamperometric study of *trans*-[MoI(NEt)(dppe)$_2$]$^+$ at 0 °C gave $k_f^I = 48 \pm 2$ s^{-1} and cyclic voltammetry gave a concordant value, 52 ± 7 s^{-1}. That release of iodide from *trans*-[MoI(NEt)(dppe)$_2$] is about 3 times as fast as is chloride loss from *trans*-[MoCl(NEt)(dppe)$_2$] is in accord with rate-determining cleavage of the molybdenum–halide bond, Scheme 2.

The rate constant k_f^{Cl} was also determined at other temperatures by chronoamperometry. Fig. 5 shows the Arrhenius plot of ln k_f^{Cl} *vs.* $1/T$ from which the activation energy E_a for the cleavage of the Mo^{III}–Cl bond in the dmf electrolyte was estimated to be 76 ± 5 kJ mol^{-1}.

Imides

The electron-transfer chemistry of imide complexes *trans*-[MoX(NH)(dppe)$_2$]$^+$ differs markedly from that of the organoimide species. Rather than Mo–X bond cleavage being the consequence of two-electron transfer, the imides give unstable amides *trans*-[MoX(NH$_2$)(dppe)$_2$], Scheme 3 (see below). The evidence for this is as follows. A typical cyclic voltammogram for the reduction of *trans*-[MoCl(NH)(dppe)$_2$]$^+$ in dmf–0.1 M [NBu$_4$][BF$_4$] at a vitreous carbon electrode is shown in Fig. 6. An irreversible reduction leads to the formation of a product which oxidises *reversibly* {*cf. irreversible* oxidation of *trans*-[Mo(NEt)(dppe)$_2$]}. The complexes *trans*-[MoX(NH)(dppe)$_2$]$^+$ (X = F, Br or I) show a parallel behaviour to that of the chloro-complex in dmf or thf electrolytes but the redox potentials for the oxidation of their products are now *related to the nature of X*, as is consistent with retention of the halide ligand in the product, *trans*-[MoX(NH$_2$)(dppe)$_2$], Table 2.

‡ Data obtained by cyclic voltammetry were analysed using the relationship $n_{apparent} = [0.4 + (k/a)]/[0.396 + 0.469\ (k/a)]$ where $a = \nu F/RT$, $F = i_p^{red}/\nu^{\frac{1}{2}} A\ C$, i_p^{red} = peak current for reduction, ν = potential scan rate, A = electrode area and C = complex concentration.

Table 2 Redox potential data for reduction of *trans*-[MoX(NH)(dppe)$_2$]$^+$ and the reversible oxidation of the intermediate *trans*-[MoX(NH$_2$)(dppe)$_2$] determined in thf–0.2 M [NBu$_4$][BF$_4$] at room temperature

X	*trans*-[MoX(NH)(dppe)$_2$]$^+$ E_p^{red}/V	*trans*-[MoX(NH$_2$)(dppe)$_2$] $E_{\frac{1}{2}}^{ox}$/V
F	−2.51	−1.85
Cl	−2.09	−1.51
Br	−2.02	−1.43
I	−2.00	−1.38

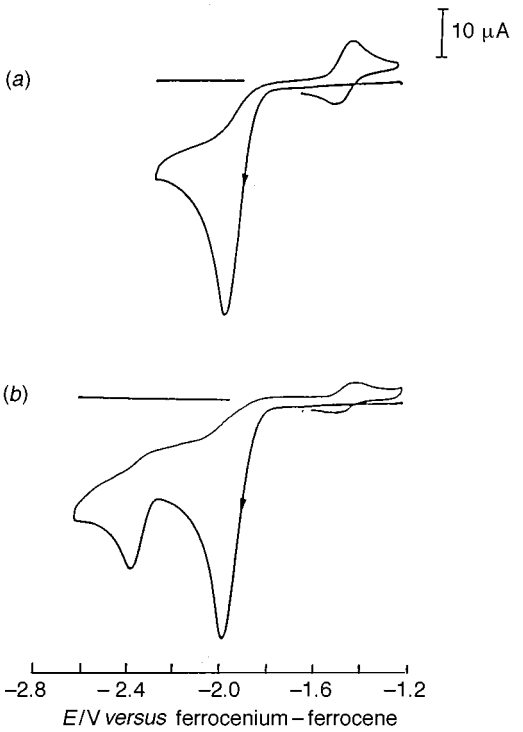

Fig. 6 Cyclic voltammograms of *trans*-[MoCl(NH)(dppe)$_2$]$^+$ showing (*a*) generation of the reversible couple *trans*-[MoCl(NH$_2$)(dppe)$_2$]–*trans*-[MoCl(NH$_2$)(dppe)$_2$]$^+$, (*b*) the reduction of *trans*-[MoCl(NH$_2$)(dppe)$_2$]. Recorded in dmf–0.1 M [NBu$_4$][BF$_4$] at a vitreous carbon electrode (area = 0.0707 cm^2) at 0 °C. Scan rate = 100 mV s^{-1}; concentration of complex = 3.56 mM

Whereas low-temperature cyclic voltammetric studies of *trans*-[MoCl(NEt)(dppe)$_2$]$^+$ allowed observation of the primary one-electron reduction product, under similar conditions we were unable to detect the corresponding formation of the molybdenum(III) imide *trans*-[MoCl(NH)(dppe)$_2$]. This irreversible behaviour also contrasts with that of the isostructural oxo-complex *trans*-[MoCl(O)(dppe)$_2$]$^+$ which undergoes reversible single-electron transfer.[11]

The difference between the electrochemical behaviour of *trans*-[MoX(NH)(dppe)$_2$]$^+$ and both that of the oxo-complex *trans*-[MoCl(O)(dppe)$_2$]$^+$ and *trans*-[MoX(NR)(dppe)$_2$]$^+$ must reside with the ability of the imide cation to act as a proton source, equation (7). The irreversibility of the reduction is thus

$$\textit{trans}\text{-[MoX(NH)(dppe)}_2\text{]}^+ + \textit{trans}\text{-[MoX(NH)(dppe)}_2\text{]} \longrightarrow \textit{trans}\text{-[MoX(N)(dppe)}_2\text{]} + \textit{trans}\text{-[MoX(NH}_2\text{)(dppe)}_2\text{]}^+ \quad (7)$$

explained by a subsequent fast chemical step whereby protonation of the N atom of *trans*-[MoX(NH)(dppe)$_2$] gives *trans*-

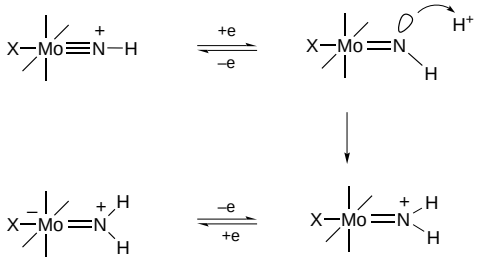

Scheme 3

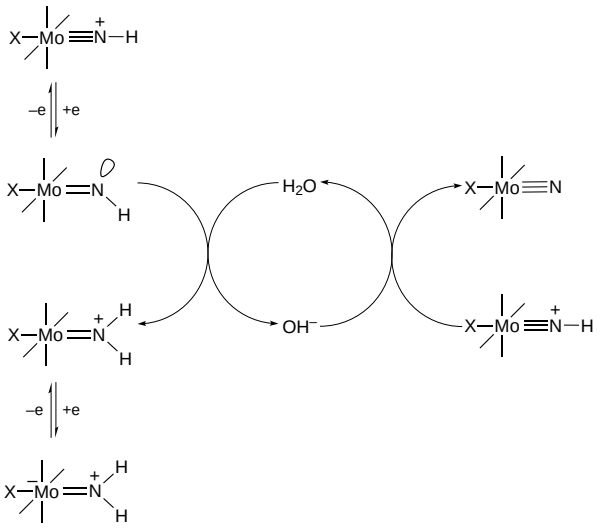

Scheme 4

$[MoX(NH_2)(dppe)_2]^+$. At the potential at which the parent imide is reduced, the amide cation will reduce to *trans*-$[MoX(NH_2)(dppe)_2]$ because $E_{\frac{1}{2}}$ $(Mo^{III/II}NH_2) \gg E_p^{red}$ $[Mo^{IV}(NH)]$, Scheme 3. Protic attack can be viewed as intercepting halide loss. Implicit in the proposed pathway is that generation of *trans*-$[MoX(NH_2)(dppe)_2]$ is accompanied by concomitant formation of the nitride *trans*-$[MoX(N)(dppe)_2]$, equation (7). The nitride is detected in the voltammetry of *trans*-$[MoCl(NH)(dppe)_2]^+$ and in that of the other halogenoimide cations. This is discussed in more detail below.

Possible mechanisms by which *trans*-$[MoCl(NH)(dppe)_2]^+$ is reduced to *trans*-$[MoCl(NH_2)(dppe)_2]$ with concomitant formation of $[MoCl(N)(dppe)_2]$ were investigated by simulation of cyclic voltammetric data using DIGISIM 2.0.[16a] Three pathways were considered: (*i*) direct transfer of a proton from *trans*-$[MoCl(NH)(dppe)_2]^+$ to *trans*-$[MoCl(NH)(dppe)_2]$; (*ii*) acid–base dissociation of *trans*-$[MoCl(NH)(dppe)_2]^+$ to give the nitride and solvated protons which then attack *trans*-$[MoCl(NH)(dppe)_2]$; (*iii*) fast protonation of *trans*-$[MoCl(NH)(dppe)_2]$ by water and deprotonation of *trans*-$[MoCl(NH)(dppe)_2]^+$ by cogenerated hydroxide, *i.e.* H_2O acts as a proton-transfer relay.

Digital simulations of the experimental cyclic voltammogram of *trans*-$[MoCl(NH)(dppe)_2]^+$ in dmf–0.1 M $[NBu_4][BF_4]$ at 0 °C were undertaken. The diffusion coefficient for the imide and those for all other metallo-species were taken as 10^{-6} cm^2 s^{-1}. The value measured by chronoamperometry for the closely related *trans*-$[Mo(N_2)_2(dppe)_2]$ was $(9 \pm 1) \times 10^{-7}$ cm^2 s^{-1} (273 K, dmf–0.1 M $[NBu_4][BF_4]$). The simulated peak current function for pathway (*i*) was about 50% of the observed experimental value. Direct protonation is probably inhibited because close encounter between the {MoNH} moieties of *trans*-$[MoCl(NH)(dppe)_2]^+$ and *trans*-$[MoCl(NH)(dppe)_2]$ is sterically unfavourable. X-Ray structural data show that the phenyl groups of the diphosphine ligands surround and extend beyond the imide group.

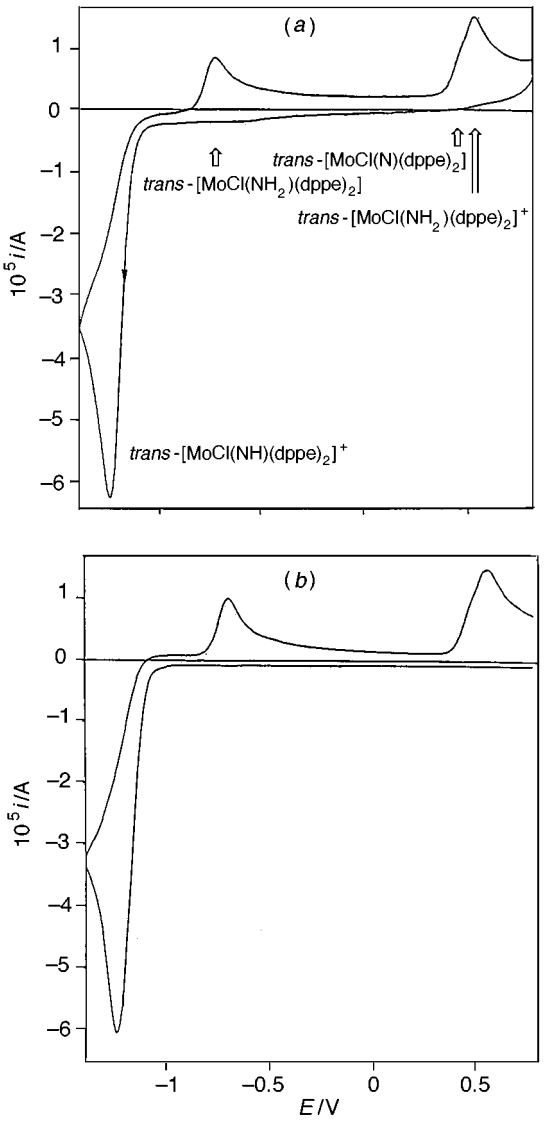

Fig. 7 Experimental (*a*) and simulated (*b*) voltammograms of *trans*-$[MoCl(NH)(dppe)_2]^+$ showing the oxidation of *trans*-$[MoCl(NH_2)(dppe)_2]^+$ and *trans*-$[MoCl(N)(dppe)_2]$. Zero on the potential axes corresponds to −0.83 V *versus* ferrocenium–ferrocene in dmf–0.1 M $[NBu_4][BF_4]$

Simulation of the voltammogram for mechanism (*ii*), attack on $[MoCl(NH)(dppe)_2]$ by solvated protons available from reversible dissociation of *trans*-$[MoCl(NH)(dppe)_2]^+$, can account for the observed peak current because the diffusion coefficient of H^+_{solv} is likely to be two or so orders of magnitude greater than that of the metallo-species. However, this mechanism demands that reversible proton dissociation from *trans*-$[MoCl(NH)(dppe)_2]^+$ is rapid. The consequence of this is that the oxidation of *trans*-$[MoCl(N)(dppe)_2]$ should be observed in the cyclic voltammetry of *trans*-$[MoCl(NH)(dppe)_2]^+$ *without excursions into the reduction process*. This is not the case: we see no evidence for oxidation of the nitride in solutions of *trans*-$[MoCl(NH)(dppe)_2]^+$ unless a base is specifically added to generate this species.

Mechanism (*iii*) involves protonation of *trans*-$[MoCl(NH)(dppe)_2]$ by water and coupled deprotonation of *trans*-$[MoCl(NH)(dppe)_2]^+$ by concomitantly generated OH^-, Scheme 4. This mechanism provides good agreement between experimental and simulated voltammetric data, Fig. 7. Sub-stoichiometric levels of water are capable of sustaining the proton-transfer catalysis. Full simulation parameters are provided in SUP 57309.

Cyclic voltammetry of *trans*-$[MoCl(NH)(dppe)_2]^+$ over a wider potential range shows the formation of the nitride *trans*-

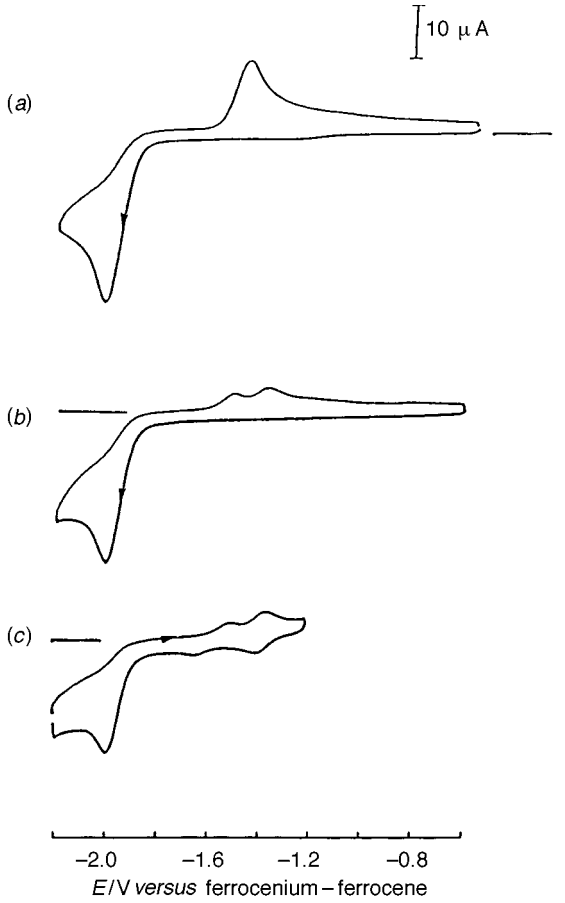

Fig. 8 Cyclic voltammograms of *trans*-[MoBr(NCH$_2$Ph)(dppe)$_2$]$^+$ in dmf–0.1 M [NBu$_4$][BF$_4$] at a vitreous carbon electrode in the absence (*a*) and in the presence of phenol (*b*), (*c*)

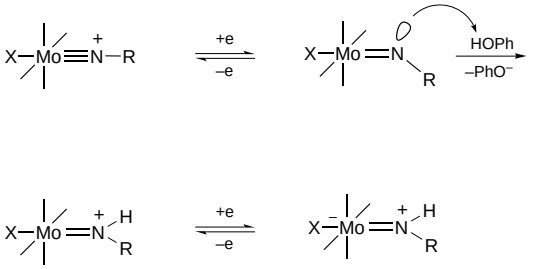

Scheme 5

[MoCl(N)(dppe)$_2$] and also the oxidation of *trans*-[MoCl(NH$_2$)(dppe)$_2$]$^+$, Fig. 7(*a*). The simulated voltammogram which includes the generation of the nitride and the oxidation processes associated with *trans*-[MoCl(NH$_2$)(dppe)$_2$]/*trans*-[MoCl(NH$_2$)(dppe)$_2$]$^+$/*trans*-[MoCl(NH$_2$)(dppe)$_2$]$^{2+}$ is also shown in Fig. 7(*b*).

Molybdenum amide complexes are rare and tend to be unstable. Recently the molybdenum(IV) dication *trans*-[Mo(OH)(NH$_2$)(dppe)$_2$]$^{2+}$ was structurally characterised by X-ray crystallography.[16b] It is isoelectronic with unstable *trans*-[MoCl(NH$_2$)(dppe)$_2$]$^{2+}$ detected in the voltammetry of *trans*-[MoCl(NH)(dppe)$_2$]$^+$, Fig. 7.

If the proposed reduction of imides to give amide intermediates is correct, we would expect reduction of alkylimides to show a parallel behaviour *in the presence of a source of protons*, *i.e.* the generation of analogous amide intermediates, *trans*-[MoX(NHR)(dppe)$_2$]. Cyclic voltammetry of *trans*-[MoCl(NR)(dppe)$_2$]$^+$ (R = Me or Et) or *trans*-[MoBr(NCH$_2$Ph)(dppe)$_2$]$^+$ in the presence of phenol results in *suppression* of the formation of *trans*-[Mo(NR)(dppe)$_2$] and the appearance of a new intermediate *which oxidises reversibly*, as illustrated by Fig. 8. This is in accord with the prediction that protonation at N intercepts halide loss and generates *trans*-[MoX(NHR)(dppe)$_2$], Scheme 5.

Table 3 Redox potentials and ^{31}P-{^{1}H} NMR data for molybdenum nitride complexes

Complex	$E_{\frac{1}{2}}^{ox}$ [a]/V	^{31}P-{^{1}H} (δ) [b]
trans-[MoF(N)(dppe)$_2$]	−0.32	−84.03, −85.15
trans-[MoCl(N)(dppe)$_2$]	−0.23	−85.50
trans-[MoBr(N)(dppe)$_2$]	−0.21	−87.75
trans-[MoI(N)(dppe)$_2$]	−0.19	−91.70

[a] Partially reversible oxidation potentials for the nitrides relative to ferrocenium–ferrocene in thf–0.2 M [NBu$_4$][BF$_4$]. [b] Chemical shifts are relative to tmp; the solvent is thf.

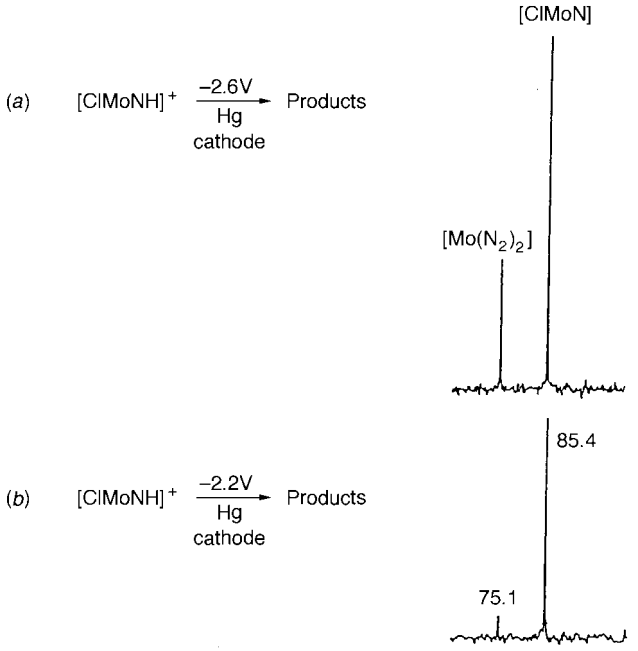

Fig. 9 The ^{31}P-{^{1}H} NMR spectra of catholyte solutions produced by reduction of *trans*-[MoCl(NH)(dppe)$_2$]$^+$ under dinitrogen at −2.6 and −2.2 V relative to ferrocenium–ferrocene at a mercury cathode. The numbers adjacent to the resonances are the chemical shifts of the products in ppm relative to tmp

Controlled-potential reduction of *trans*-[MoCl(NH)(dppe)$_2$]$^+$ ($E_{applied}$ = −2.2 V *versus* ferrocenium–ferrocene; thf–0.2 M [NBu$_4$][BF$_4$] or dmf–0.1 M [NBu$_4$][BF$_4$]) is an overall one-electron process at a mercury-pool cathode and gives *trans*-[MoCl(N)(dppe)$_2$] in 90% yield, as shown by the ^{31}P-{^{1}H} NMR spectrum of Fig. 9, together with *trans*-[Mo(N$_2$)$_2$(dppe)$_2$] and a trace of ammonia. Evidently the amide *trans*-[MoCl(NH$_2$)(dppe)$_2$] is not a stable product on the preparative time-scale (*ca.* 15 min) but is an intermediate on an overall one-electron pathway to the nitride *trans*-[MoCl(N)(dppe)$_2$]. The behaviour of other *trans*-[MoX(NH)(dppe)$_2$]$^+$ under these conditions is quite similar; *trans*-[MoX(N)(dppe)$_2$] (X = F, Br or I) are shown to be the major metal products by cyclic voltammetry and ^{31}P-{^{1}H} NMR spectroscopy, Table 3. Attempts to prepare *trans*-[MoX(NH$_2$)(dppe)$_2$] by low-temperature electrolysis for spectroscopic studies were unsuccessful.

Loss of dihydrogen from *trans*-[MoX(NH$_2$)(dppe)$_2$] could explain the formation of *trans*-[MoX(N)(dppe)$_2$], equation (8).

$$\textit{trans}\text{-[Mo(NH}_2\text{)(dppe)}_2\text{]} \longrightarrow \textit{trans}\text{-[Mo(N)(dppe)}_2\text{]} + \text{H}_2 \quad (8)$$

Analysis by gas chromatography of the head-space in the

Table 4 Yields of products of reduction of imide complexes[a]

Imide complex	Products (yields in mol% mol^{-1} imide)
trans-$[MoF(NH)(dppe)_2]^+$	NH_3 (10.5), *trans*-$[Mo(N_2)_2(dppe)_2]$ (22), *trans*-$[MoF(N)(dppe)_2]$ (78)
trans-$[MoCl(NH)(dppe)_2]^+$	NH_3 (15.0), *trans*-$[Mo(N_2)_2(dppe)_2]$ (27), *trans*-$[MoF(N)(dppe)_2]$ (73)
trans-$[MoBr(NH)(dppe)_2]^+$	NH_3 (14.5), *trans*-$[Mo(N_2)_2(dppe)_2]$ (22), *trans*-$[MoF(N)(dppe)_2]$ (65)[b]
trans-$[MoI(NH)(dppe)_2]^+$	NH_3 (6.0), *trans*-$[Mo(N_2)_2(dppe)_2]$, free phosphine, unidentified products

[a] Exhaustive controlled-potential electrolysis at potentials *ca.* $(E_p^{red} - 0.1)$ V on a mercury-pool cathode in thf–0.2 M $[NBu_4][BF_4]$. [b] About 13 mol% *trans*-$[MoCl(N)(dppe)_2]$ is also formed by scavenging of Cl^-.

electrolysis cell after reduction of *trans*-$[MoCl(NH)(dppe)_2]^+$ (vitreous carbon; dmf–0.1 M $[NBu_4][BF_4]$, 298 K) confirmed the generation of H_2 in significant amounts (*ca.* 20–30 mol%). That the formation of dihydrogen is not stoichiometric suggests other decomposition pathways must also be involved, possibly 2H transfer to solution species, but this has not been investigated.

The decomposition of *trans*-$[MoCl(NH_2)(dppe)_2]$ is reminiscent of the thermal conversion of *trans*-$[MoCl(CNH_2)(dppe)_2]$ to the cyanide *trans*-$[MoCl(CN)(dppe)_2]$[17] whereby the aminocarbyne acts as a 2H source. In both cases, the driving force is presumably the generation of a triple bond, Mo≡N and C≡N respectively. Perhaps a closer analogy is the conversion of a W^{IV}–CH_3 group into the W^{VI}≡CH group by dihydrogen loss,[18] the driving force again being attributable to the formation of the multiple metal–carbon bond. It is possible that these dihydrogen-elimination processes occur by a common mechanism. The methyl to methylidyne conversion has been suggested to occur by α elimination;[18] although dihydrogen is detected the yield has not been quantified. A pathway which does not involve metal hydride formation, but coupling at the light atom, is a possibility.

The rate of decomposition of *trans*-$[MoCl(NH_2)(dppe)_2]$ to the nitride is relatively slow on the cyclic voltammetric timescale; good correspondence between experimental and simulated voltammograms was obtained when the global first-order rate constant for decay of the amide was taken to be 0.05 ± 0.03 s^{-1} at 0 °C, Fig. 7. It is the relatively long life of the amide which allows its participation in further electron-transfer chemistry which leads to the formation of ammonia.

Formation of ammonia and amines

The intermediate *trans*-$[MoCl(NH_2)(dppe)_2]$ undergoes reduction at a potential negative of the primary process for the reduction of *trans*-$[MoCl(NH)(dppe)_2]^+$, Fig. 6. Controlled-potential electrolysis of *trans*-$[MoCl(NH)(dppe)_2]^+$ (mercury-pool; thf–0.2 M $[NBu_4][BF_4]$) was therefore carried out at $E_{applied} = -2.6$ V *versus* ferrocenium–ferrocene, a potential which accommodates the reduction of the amide intermediate. This changes the product distribution from that observed at potentials close to E_p^{red} for the parent imide. Ammonia and the dinitrogen complex *trans*-$[Mo(N_2)_2(dppe)_2]$ are now formed in significant amounts. The ratio of the metal products (dinitrogen complex : nitride) changes from *ca.* 1 : 10 to *ca.* 1 : 3 [compare Fig. 9, (*a*) and (*b*)]. The yield of ammonia increases from <1 to 15 mol% mol^{-1} {*trans*-$[MoCl(NH)(dppe)_2]^+$} and the overall charge consumed increases to 1.2 F mol^{-1} complex. The ratio of the yields of metal products are in reasonable accord with the global stoichiometry of equation (9). The yield of ammonia

$$4\ \textit{trans}\text{-}[MoX(NH)(dppe)_2]^+ + 4e + 2N_2 \longrightarrow 3\ \textit{trans}\text{-}[MoX(N)(dppe)_2] + \textit{trans}\text{-}[Mo(N_2)_2(dppe)_2] + NH_4^+ + X^- \quad (9)$$

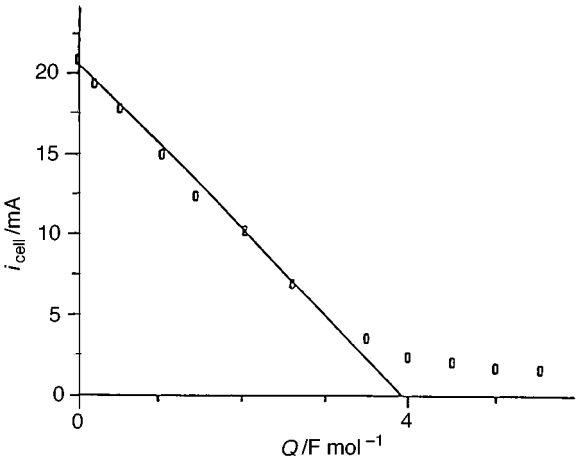

Fig. 10 Current *versus* charge passed plot for reduction of *trans*-$[MoBr(NCH_2Ph)(dppe)_2]^+$ at 0 °C in dmf–0.1 M $[NBu_4][BF_4]$ at a mercury-pool cathode. $E_{applied} = -2.31$ V

is *ca.* 60% of theoretical based on this stoichiometry and the *n* value is near the theoretical value of 1.25 expected from equation (9) and one-electron discharge of ammonium to ammonia. The behaviour of other *trans*-$[MoX(NH)(dppe)_2]^+$ (X = F, Br or I) is broadly similar except that reduction of the iodide leads to decomposition with the liberation of free phosphine, Table 4.

As discussed in the preceding section, *trans*-$[MoX(NHR)(dppe)_2]$ is generated from the organoimide cations in the presence of phenol. This provides a route to amines. Thus controlled-potential electrolysis of *trans*-$[MoX(NR)(dppe)_2]^+$ [R = Me or Et, X = Cl; R = $PhCH_2$ or PhCH(Me), X = Br] in the presence of phenol (mercury-pool; thf–0.2 M $[NBu_4][BF_4]$) is an overall four-electron process and leads to the liberation of the free amine and the generation of *trans*-$[Mo(N_2)_2(dppe)_2]$. Fig. 10 illustrates a typical current *versus* charge passed plot. Cyclic voltammetry on the catholyte solutions at the end of electrolysis showed that the dinitrogen complex is formed in yields of 80–90%. The amines $PhCH_2NH_2$ and $PhCH(Me)NH_2$ were identified by ^1H NMR, IR spectroscopy and TLC and are formed in yields of *ca.* 70 mol%. Methylamine was formed in *ca.* 50 mol% yield and was identified and estimated colorimetrically.

Certain organoimides show a parallel in their reduction pattern to that of the imides. Whereas the latter act overall as sacrificial N-acids supplying protons for the formation of ammonia, alkylimides *trans*-$[MoX(NCH_2CO_2R)(dppe)_2]^+$ (X = Cl or Br, R = Me or Et) perform the same task by acting as α C-acids. Thus the conjugate base *trans*-$[MoX(NCHCO_2Me)(dppe)_2]$, glycine methyl ester, and *trans*-$[Mo(N_2)_2(dppe)_2]$ are produced by electroreduction under molecular nitrogen.[6]

Mechanism of formation of dinitrogen complexes

Cyclic voltammetric information on the mechanism of dinitrogen complex formation from the amide intermediates is masked because the electron-transfer chemistry is fast. However, earlier electrochemical studies on the formation of dinitrogen complexes by reduction of molybdenum(II) halide precursors provide some insight into possible pathways.[19] We make the assumption that reduction and protonation of the amide intermediates initially gives molybdenum(I) amine complexes according to Scheme 6. Neutral donor ligands are labile at low-valent *trans*-$\{Mo(dppe)_2\}$ sites and it is likely that the amine rapidly dissociates from *trans*-$[MoX(NH_2R)(dppe)_2]$ to be replaced by dinitrogen. As established from studies of the electrochemistry of complexes *trans*-$[MoX_2(dppe)_2]$ (X = halide), the binding of a π-acid ligand promotes diffusion-

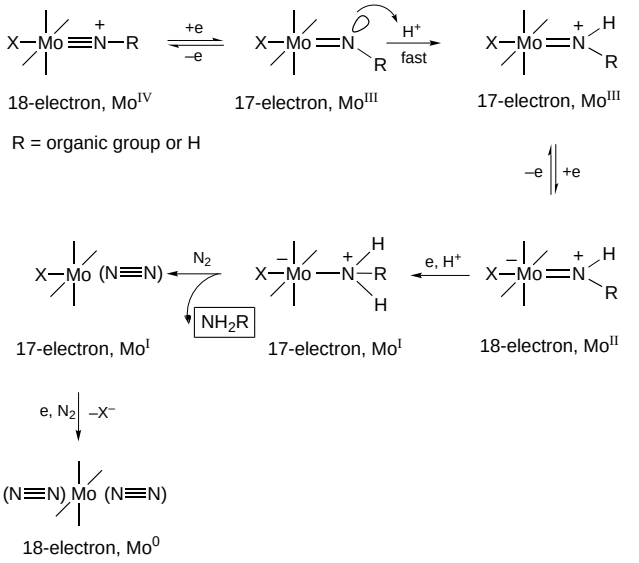

Scheme 6

controlled reduction of 17-electron *trans*-$[MoX(N_2)(dppe)_2]$ to the 18-electron anion which then loses the halide ligand, thus allowing co-ordination of a second dinitrogen molecule, Scheme 6.

Conclusion

The electrochemical reduction of the molybdenum(IV) alkylimides *trans*-$[MoX(NR)(dppe)_2]^+$ proceeds by two pathways. In the *absence* of a source of protons, moderately stable five-co-ordinate molybdenum(II) imides are formed *via* an initial single-electron transfer followed by rate-determining loss of the *trans*-halide ligand and an additional electron transfer. In the *presence* of a source of protons, molybdenum–halide bond cleavage is intercepted by protonation at N which gives an amide intermediate. Further electron-transfer chemistry liberates amines and yields a dinitrogen complex in an overall four-electron process. Molybdenum(IV) imides *trans*-$[MoX(NH)(dppe)_2]^+$ are reduced to amide intermediates with the parent imide cation providing the source of protons and water probably acts as a proton-transfer relay. The amide has two fates; it is either converted into a nitride by hydrogen loss or, at a potential which encompasses its further reduction, yields ammonia and dinitrogen complex.

Experimental

All manipulations were carried out under an inert atmosphere of dinitrogen or argon using Schlenk techniques. Solvents were freshly distilled from appropriate drying agents under dinitrogen. Complexes *trans*-$[MoX(NH)(dppe)_2][Q]$ (X = halide, Q = X or BPh_4)[20] and *trans*-$[MoX(NR)(dppe)_2][Q]$ (X = halide, R = organic group, Q = X or BPh_4)[6] were prepared from the nitride precursors by the literature methods.[6,20,21]

The NMR measurements, were made on a JEOL FX90Q instrument. Gas chromatography measurements (dihydrogen) were made on a Philips PU 4400 chromatograph interfaced with a PU 4815 integrator. The column was 2 m × 1/8 in internal diameter stainless steel packed with molecular sieves (80–100 mesh) and run at 60 °C with argon as the carrier gas; the injector and thermal conductivity detector heads were held at 100 °C.[22] Gas samples were taken from the head-space above the electrolyte in an H-type cell *via* a septum cap; the head-space above the anolyte and catholyte chambers was interconnected. Injection of known volumes of dihydrogen into the head-space of the cell was used for standardisation.

Controlled-potential electrolyses were carried out in an H-type cell with a mercury-pool or vitreous carbon working electrode as described previously.[6,23] Ammonia formed by electrolysis was determined by the indophenol test using the procedure described earlier.[23] Methylamine was estimated colorimetrically using 2,4-dinitrofluorobenzene.[24]

Cyclic voltammetric output from a EG and G PAR model 273 potentiostat was collected on a Viglen Genie PCi P5/166 instrument running EG and G PAR M270 sofware and imported into DIGISIM 2.0 software for comparison with simulated data. All simulations were performed with the pre-equilibria condition enabled in the program. Experimental data were *not* corrected for background faradaic current, charging current or *iR* drop. Charging current and *iR* drop were incorporated in the simulations.

Acknowledgements

We thank the University of Malaya for providing an Overseas Postgraduate Research Scholarship (to Y. A.), the Université de Bretagne Occidentale for supporting Florence Volant's DEA research stage in the Nitrogen Fixation Laboratory (NFL), and Instituto Nacional de Investigaçao Científica for providing Antonio Fonseca with funds to undertake part of his post-graduate research work at NFL. The British Council is thanked for providing travel funds and the BBSRC is gratefully acknowledged for supporting the work and providing research facilities.

References

1 M. Hidai and Y. Ishii, *J. Mol. Catal.*, 1996, **107**, 105; M. Hidai and Y. Mizobe, *Chem. Rev.*, 1995, **95**, 1115; Y. Mizobe, Y. Ishii and M. Hidai, *Coord. Chem. Rev.*, 1995, **139**, 281.
2 T. Yoshida, T. Adachi, T. Ueda, M. Kaminaka, N. Sasaki, T. Higuchi, T. Aoshima, I. Mega, Y. Mizobe and M. Hidai, *Angew. Chem., Int. Ed. Engl.*, 1989, **28**, 1040.
3 J. Chatt, J. R. Dilworth and R. L. Richards, *Chem. Rev.*, 1978, **78**, 589; R. A. Henderson, G. J. Leigh and C. J. Pickett, *Adv. Inorg. Radiochem.*, 1983, **27**, 197; C. J. Pickett, M.-L. Abasq and S. K. Ibrahim, in *Novel Trends in Electroorganic Synthesis*, ed. S. Torii, Kondansha, Japan, 1995, pp. 231–234; C. J. Pickett, in *Molecular Electrochemistry of Inorganic, Bioinorganic and Organometallic Compounds*, eds. A. J. L. Pombeiro and J. A. McCleverty, NATO ASI Series C, 1993, vol. 385, pp. 357–380.
4 Y. Ishii, H. Miyagi, S. Jitsukuni, H. Seino, B. S. Harkness and M. Hidai, *J. Am. Chem. Soc.*, 1992, **114**, 9890.
5 H. Seino, Y. Ishii and M. Hidai, *J. Am. Chem. Soc.*, 1994, **116**, 7433.
6 S. A. Fairhurst, D. L. Hughes, S. K. Ibrahim, M.-L. Abasq, J. Talarmin, M. A. Queiros, A. Fonseca and C. J. Pickett, *J. Chem. Soc., Dalton Trans.*, 1995, 1873.
7 G. E. Bossard, T. A. George, R. K. Lester, R. C. Tisdale and R. L. Turcotte, *Inorg. Chem.*, 1985, **24**, 1129.
8 T. Yoshida, T. Adachi, M. Kaminaka and T. Ueda, *J. Am. Chem. Soc.*, 1988, **110**, 4872.
9 W. Hussain, G. J. Leigh and C. J. Pickett, *J. Chem. Soc., Chem. Commun.*, 1982, 747; R. A. Henderson, G. J. Leigh and C. J. Pickett, *J. Chem. Soc., Dalton Trans.*, 1989, 425; D. L. Hughes, D. J. Lowe, C. J. Macdonald, M. Y. Mohammed and C. J. Pickett, *Polyhedron*, 1989, **8**, 1653; D. L. Hughes, M. Y. Mohammed and C. J. Pickett, *J. Chem. Soc., Chem. Commun.*, 1989, 1399; *J. Chem. Soc., Dalton Trans.*, 1990, 2013; A. Hills, D. L. Hughes, C. J. Macdonald, M. Y. Mohammed and C. J. Pickett, *J. Chem. Soc., Dalton Trans.*, 1991, 121; R. A. Henderson, S. K. Ibrahim and C. J. Pickett, *J. Chem. Soc., Chem. Commun.*, 1993, 392.
10 D. L. Hughes, S. K. Ibrahim, C. J. Macdonald, H. Moh'd Ali and C. J. Pickett, *J. Chem. Soc., Chem. Commun.*, 1992, 1762.
11 D. L. Hughes, M. Y. Mohammed and C. J. Pickett, *J. Chem. Soc., Chem. Commun.*, 1988, 1119.
12 C. J. Pickett, *JBIC*, 1996, **1**, 606.
13 V. V. Strelets and C. J. Pickett, *Elektrokhimiya*, 1994, **30**, 1023.
14 W. E. Geiger, P. H. Reiger, B. Tulyathan and M. D. Rausch, *J. Am. Chem. Soc.*, 1984, **106**, 7000.
15 G. S. Alberts and I. Shain, *Anal. Chem.*, 1963, **35**, 1859; A. J. Bard and L. R. Faulkner, *Electrochemical Methods*, Wiley, New York, 1980, p. 462.
16 (*a*) M. Rudolph and S. W. Feldberg, DIGISIM 2.0, Bioanalytical Systems Inc., West Lafayette, IN, 1994; (*b*) T. Adachi, D. L. Hughes, S. K. Ibrahim, S. Okamoto, C. J. Pickett, N. Yabanouchi and T. Yoshida, *J. Chem. Soc., Chem. Commun.*, 1995, 1081.

17 D. L. Hughes, S. K. Ibrahim, H. Moh'd Ali and C. J. Pickett, *J. Chem. Soc.*, *Chem. Commun.*, 1994, 425.
18 K.-Y. Shih, K. Totland, S. W. Siedel and R. R. Schrock, *J. Am. Chem. Soc.*, 1994, **116**, 121 03.
19 T. I. Al-Salih and C. J. Pickett, *J. Chem. Soc.*, *Dalton Trans.*, 1985, 1255.
20 P. C. Bevan, J. Chatt, J. R. Dilworth, R. A. Henderson and G. J. Leigh, *J. Chem. Soc.*, *Dalton Trans.*, 1982, 821.
21 J. Chatt and J. R. Dilworth, *J. Chem. Soc.*, *Chem. Commun.*, 1975, 983; *J. Indian Chem. Soc.*, 1977, **54**, 13.
22 R. A. Henderson and K. Oglieve, *J. Chem. Soc.*, *Dalton Trans.*, 1996, 3397.
23 C. J. Pickett, K. S. Ryder and J. Talarmin, *J. Chem. Soc.*, *Dalton Trans.*, 1986, 1453.
24 D. T. Dubin, *J. Biol. Chem.*, 1960, **235**, 783.

Received 28*th July* 1997; *Paper* 7/05441F